1996

Simple retrofittable long-range x-y translation system for scanned probe microscopes

Walter Fox Smith
Haverford College, wsmith@haverford.edu

M. C. Abraham

J. M. Sloan

M. Switkes

Simple retrofittable longrange x–y translation system for scanned probe microscopes

W. F. Smith, M. C. Abraham, J. M. Sloan, and M. Switkes

Citation: Rev. Sci. Instrum. **67**, 3599 (1996); doi: 10.1063/1.1147065
View online: http://dx.doi.org/10.1063/1.1147065
View Table of Contents: http://rsi.aip.org/resource/1/RSINAK/v67/i10
Published by the American Institute of Physics.

Simple retrofittable long-range $x-y$ translation system for scanned probe microscopes

W. F. Smith,[a)] M. C. Abraham, J. M. Sloan, and M. Switkes[b)]
Physics Department, Haverford College, Haverford, Pennsylvania 19041

(Received 9 February 1996; accepted for publication 29 July 1996)

A simple, reliable system for long-range translation of scanned probe microscopy (SPM) samples is described. This system could easily be retrofitted to many existing SPMs. The sample is held magnetically onto the scan piezo tube, and is translated by stick-slip motion. The system is very reliable, and provides controllable step size ranging from 20 nm to 1 μm. Three stick-slip drive wave forms are described and tested: sawtooth, cycloid, and an ''improved'' cycloid based on the resonance curve of a harmonic oscillator. Computer simulations of the stick-slip process are presented, and are in good agreement with experiment. Together, the experiments and simulations demonstrate that it is essential to consider the resonant response of the piezo when evaluating drive wave forms. © *1996 American Institute of Physics.* [S0034-6748(96)05010-1]

I. BACKGROUND

For much of the research performed to date using scanned probe microscopes (SPMs), the images and spectroscopy presented are meant to be representative of a uniform macroscopic sample; the precise $x-y$ location of the scan on the sample is unimportant, since all areas of the sample are nominally identical. However, there is an increasing need to image a particular site on the sample surface, or, for nanofabrication using scanned probes, to fabricate a structure at a unique site. Achieving these goals requires (1) a system for translating the tip relative to the sample (or vice versa) over macroscopic distances with high precision and (2) a relatively wide-field microscope that allows real-time viewing of the tip and sample so as to allow positioning of the tip over the desired site.

Many commercial SPMs feature $x-y$ translation of the sample using micrometer-screws. While this method is certainly convenient and precise, it necessarily adds massive elements to the mechanical loop between tip and sample, which lowers the SPM resonant frequency, thereby diminishing the effectiveness of the vibration isolation.[1] Many $x-y$ translation systems previously described[2,3] provide admirable performance, but are fairly complex, and must essentially be part of the initial design of the SPM. In this article, we describe a very simple system for long range $x-y$ translation that will be easy to retrofit onto most existing SPMs, yet one that provides the necessary precision as well as excellent reliability and high translation speed (when desired). The system we describe is inspired in part by that of Asenjo and co-workers;[4] their system has the advantage of being completely free of magnets, and therefore suitable for use in a scanning electron microscope, whereas the system described here is simpler and less massive.

II. OVERVIEW OF DESIGN

As shown schematically in Fig. 1, the sample is affixed to a μ-metal plate that is held magnetically against a stainless steel washer attached to the piezo scan tube. (Details of the construction will be described below.) Throughout this discussion, we assume that the plane of the sample is vertical, as shown. This is a more challenging geometry than a horizontal sample, since a vertical sample must be moved against the force of gravity for $+y$ motion.

Motion of the sample relative to the scan tube is accomplished by a stick-slip cycle. For example, to move the sample to the left, a cycloidal wave form[5] such as that shown in Fig. 2 is applied to the left piezo electrode. Simultaneously, an identical wave form with inverted polarity is applied to the right electrode. The lateral translation of the piezo in response to such symmetrically applied voltage is approximately linear, so the vertical scale can be approximately interpreted as the lateral position of the piezo. Therefore, the acceleration applied to the piezo is given by the curvature (second derivative) of this curve.

At first (phase 1 in the diagram) the piezo and sample are gently accelerated to the left. In the noninertial reference frame of the sample, there is a small pseudoforce to the right during this phase; however, the friction between the μ-metal plate and the washer to which it is magnetically held is large enough to prevent relative motion. In phase 2, the direction of motion is reversed, resulting in a large acceleration of the piezo to the right. In the noninertial frame of the sample, this corresponds to a large pseudoforce to the left, large enough to exceed the force of friction holding the sample in place, resulting in motion of the sample to the left, relative to the piezo tube. Finally, in phase 3, additional gentle leftward acceleration brings the piezo momentarily back to rest, ready for a new cycle.

To move the sample to the right, one can simply switch the wave forms between left and right electrodes, i.e., one can apply the wave form shown in Fig. 2 to the right electrode-and the opposite polarity version to the left electrode. Alternatively, one can slowly ramp the voltage to the desired peak value on the left electrode, and apply a downward pointing cusp (with minimum voltage of 0). (Meanwhile, as usual, one applies the identical but polarity-reversed wave form to the right electrode.) We have tested both methods, and they are equally effective. Throughout the

[a)]Electronic mail: wsmith@haverford.edu
[b)]Current address: Physics Dept., Stanford University, Stanford, California 94305.

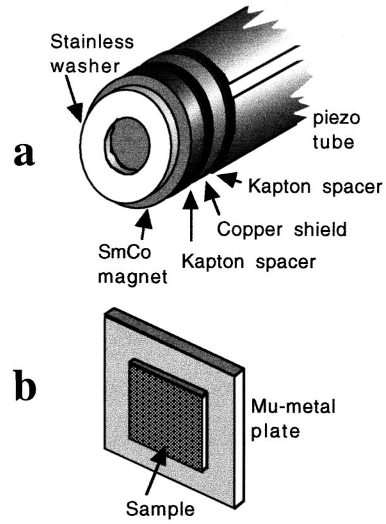

FIG. 1. Schematic drawings of (a) the magnetic hold-down arrangement at the end of the scan piezo and (b) the sample mounting arrangement. All parts shown are held together with epoxy, although the sample is held to the μ-metal plate with silver paint. It should also be possible to hold the sample to the μ-metal plate using epoxy or spring clips. All construction materials are ultrahigh vacuum compatible, except for the silver paint and the ultramini-coax used to deliver the bias voltage (used for scanning tunneling microscopy) to the disk magnet.

procedure, to avoid any danger of depoling the piezo, the center electrode is held at a constant -100 V. (Our piezo tube, like most, is poled with the outer electrodes positive relative to the inner.)

III. DESIGN CONSIDERATIONS

To avoid slippage of the sample during a conventional scan (and during phases 1 and 3 of Fig. 2), it is desirable to use both a large hold-down force and a large frictional force between the μ-metal plate and the surface on which it slides. However, if the frictional force is too high, the pseudoforce generated during phase 2 will be insufficient to move the sample. The pseudoforce is given by $F_{\text{pseudo}}=-ma$, where m is the mass of the sample plus μ-metal plate, and a is the acceleration of the piezo. Obviously, one way to increase the pseudoforce is simply to increase the mass of the sample or the μ-metal plate. However, this has the undesirable effect of lowering the resonant frequency of the tip-to-sample mechanical loop (thereby decreasing the effectiveness of vibration isolation[1]). Also, once the weight of the sample becomes comparable to the frictional force, further increases in sample mass are not helpful, since they increase both F_{pseudo} and the total force that it must overcome (=frictional force plus weight) to move the sample upward.

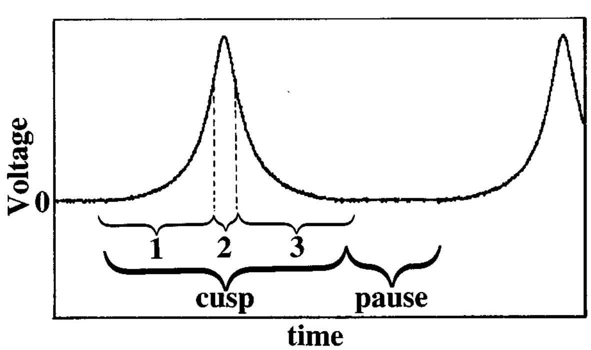

FIG. 2. A possible stick-slip drive wave form. The wave form chosen for display here (improved cycloid, $Q=4$) shows the various phases clearly, but was not used for any experiments.

Therefore, instead of increasing m, it is preferable to maximize the acceleration applied to the piezo, a. The maximum value of this acceleration is determined (1) by the maximum amplitude of voltage wave form that can be applied to the piezo and (2) by the characteristic width of the acceleration cusp in phase 2. In principle, the width of the cusp can be reduced to zero, but the actual experimental width is roughly determined either by the mechanical resonance frequency of the piezo or by the $f_{3\ \text{dB}}$ of the electronics driving the piezo, whichever is lower. For most SPMs, the mechanical resonance frequency, f_{res}, (usually several kHz) is lower.

For most existing SPMs, neither the maximum voltage nor the piezo resonance frequency can be easily changed. Therefore, assuming the cycloid wave form is properly generated, there is little that can be done to increase the maximum piezo acceleration.

Therefore, to insure $F_{\text{pseudo}} \geqslant F_{\text{friction}}$, one may need to reduce F_{friction}. So long as the sum of the gravitational force, the pseudoforces generated by unwanted vibrations, and the pseudoforces generated during a scan are less than F_{friction}, such a reduction has no deleterious effects.

Estimates of typical building vibrations vary from[6] 6×10^{-5} g to about[2] 4×10^{-3} g, where g is the acceleration of gravity. Even in a light manufacturing environment, the vibration[7] is less than 0.01 g. Most SPMs are mounted on a vibration isolation stage, reducing this figure even further. So, it is clear that, if the sample is stable against the acceleration of gravity, it will certainly not be moved by building vibrations.

One might be concerned that the pseudoforces generated during a conventional imaging scan would be quite large, since it is common to use a triangular wave for driving the piezo raster, and since, in principle, the acceleration at the triangle apex is infinite. However, in fact, as is the case for the cycloid cusp, the velocity reversal that occurs at the triangle apex is not instantaneous but, rather, occurs over a time scale of roughly $1/f_{\text{res}}$. (Our simple computer simulations indicate that the maximum acceleration is given approximately by $5\Delta v f_{\text{res}}$ where Δv is the change in velocity at the cusp apex, and is only weakly dependent on the damping assumed.) Since the wave forms used for stick-slip motion have *much* higher Δv than those used for scans, it is easy to ensure that no unintended motion will occur during scans. For example, for a 10 Hz scan (faster than is used by most experimenters for large scans) using a triangular wave form for the raster, with 1 μm amplitude, using a piezo with resonance frequency 15 kHz, the maximum acceleration would be about 0.3 g.

IV. CONSTRUCTION DETAILS

A samarium–cobalt disk magnet [0.63-mm-thick$\times$0.63 cm diameter, magnetized through the thickness (Magnet

Sales, Culver City, CA)] is epoxied to the end of the piezo tube. The magnet is shielded from the electric fields of the piezo electrodes by a grounded copper annulus. The annulus and the magnet are electrically isolated by kapton spacers [0.13-mm-thick, type HN (Dupont Corp., Circleville, OH)], as shown in Fig. 1(a). The bias voltage (for scanning tunneling microscopy) is applied to the disk magnet via an ultramini-coax cable (Lakeshore Cryotronics, Westerville, OH) that runs through the center of the piezo tube. As will be discussed below, we attached a stainless steel washer (size M3, 0.5 mm thickness) to the disk magnet to reduce the frictional force.

The sample is affixed to a 0.4-mm-thick, 1.2-cm-sq μ-metal plate (Amuneal Manufacturing, Philadelphia, PA), either with conductive epoxy, silver paint, or spring clips. (For all tests reported here the sample was attached with silver paint.) In operation, the backside of the μ-metal plate is held magnetically against the stainless washer.

For the measurements reported here, the frictional force was reduced (1) by sanding the back of the μ-metal plate with 600 grit sandpaper and (2) by adding the stainless steel washer shown in Fig. 1(a) between the μ-metal plate and the disk magnet. This washer provided both a smooth surface and a reduced the hold-down force (thereby also reducing the frictional force). The measured static frictional force was 0.065 ± 0.005 N, which is about ten times the force of gravity on our sample. Therefore (by the arguments above) this frictional force provides more than 1000 times the force required to hold the sample in place against building vibrations and more than 30 times the force required to hold it in place even during a rather rapid imaging scan. However, the frictional force could be increased by a factor of 5 and still allow very reliable stick-slip motion. The combined mass of sample plus μ-metal plate was 0.626 g.

Our piezo tube is made of PZT-4, with 0.5 mm wall thickness, 0.64 cm o.d., and 1.27 cm length (Staveley Sensors, East Hartford, CT).

The only subtle point in getting the system to work is that the μ-metal plate must be larger than the stainless washer; as soon as one edge of the plate comes into contact with the washer, motion in that direction stops. This has the benefit that it is impossible to accidentally drive the sample off the piezo. (The sample does not get stuck in this situation; one can still drive it back in the other direction.)

V. RESULTS

We evaluated three excitation wave forms: the standard cycloid[5] (see Fig. 4), the sawtooth wave form used in many stick-slip systems, and an ''improved'' cycloid. The cycloid is admirable in that, in principle, it provides the maximum acceleration in one direction and the minimum in the other. (In contrast, the sawtooth has very high acceleration in both directions because it has a sharp positive-curvature corner as well as a sharp negative-curvature corner.) However, as already discussed, the maximum acceleration is actually determined by the resonance frequency of the piezo tube. Therefore, it may be useful to have control over the curvature of the cusp. One mathematical function that is cusplike yet allows control over the cusp sharpness is the resonance curve

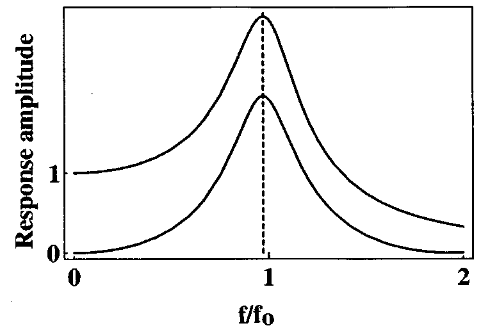

FIG. 3. Mirroring procedure used to construct the ''improved'' cycloid. The upper curve is the response of a damped, driven harmonic oscillator. The vertical axis is the response amplitude relative to the excitation amplitude and f_0 is the undamped resonance frequency. Note that the maximum of the resonance curve is slightly to the left of $f/f_0=1$. The lower curve shows the improved cycloid that is formed by mirroring the left half of the resonance curve.

(response versus frequency) of a damped, driven harmonic oscillator. The sharpness of the cusp is adjusted by changing the quality factor Q. However, this resonance curve is not symmetrical about the cusp. Therefore we use only the left half of the resonance curve, and mirror it to achieve a symmetrical wave form, as shown in Fig. 3. The mathematical form of the resonance curve is

$$y=\frac{1}{\sqrt{(1-z^2)^2+\dfrac{4z^2}{4Q^2+2}}},$$

where $z=f/f_0$ and f_0 is the natural frequency of the harmonic oscillator without damping. To achieve a wave form that has $y(0)=0$, we subtract 1 from the above. Then, to allow variation of Q without affecting the amplitude of the wave form, the curve is normalized by multiplying by $\sqrt{Q^2+(1/2)}$. To achieve proper mirroring, it is important to note that the maximum in the resonance curve does not occur at f_0 (i.e., at $z=1$), nor does it occur at the natural oscillation frequency of the damped (undriven) oscillator. Rather, the maximum occurs at

$$z=\sqrt{1-\frac{1}{1+2Q^2}}.$$

For each of the three wave forms, measurements were made with a wave train of 500 or 1000 cusps so as to give enough motion to be readily measured by an optical microscope. A standard cusp-to-cusp repeat frequency of 813 Hz was used for the wave train for all wave forms (sawtooth, standard cycloid, and improved cycloid). For the improved cycloid, we used a standard time span of 614 μs for each cusp, with a pause of 614 μs between each cycloid (giving a total repeat time of 1.228 ms, which corresponds to the 813 Hz repeat frequency).

It is desirable that a stick-slip wave form produce repeatable motion at a low amplitude. (This, for example, allows use of higher frictional forces or less expensive amplifiers.) We measured the minimum drive wave form amplitude required for movement (the ''motion threshold'') by observing

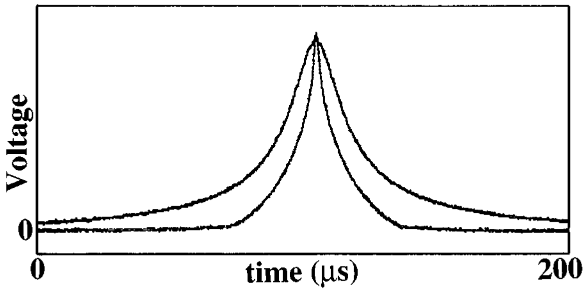

FIG. 4. Cycloidal wave forms used for Table I. The outer curve is an improved cycloid with $Q=20$ and cusp width of 614 μs. The inner curve is a standard cycloid with cusp width of 82 μs.

the sample motion with an optical microscope. For the improved cycloid, the lowest motion threshold was found for Q in the range 20–25. We used $Q=20$ for all subsequent measurements. This wave form is shown as the top trace in Fig. 4.

For comparison, we varied the width of the standard cycloid cusp, and found that the minimum motion threshold occurred at a width of 80 ± 20 μs. This standard cycloid is shown as the bottom trace of Fig. 4.

The motion threshold was measured at five different sites for each of the three wave forms. The results were quite consistent from site to site and are summarized in Table I. The improved cycloid has a threshold that is slightly lower than the best standard cycloid. (The uncertainty in Table I is largely due to site-to-site variations; at every site, the improved cycloid had a slightly lower threshold than the standard cycloid.) Surprisingly, the sawtooth had a considerably lower threshold than either of the other wave forms.

Presumably there is a minimum speed of drive wave form amplifier needed for reliable stick-slip motion, however, our results show that the requirements are modest. The results reported here are for a moderately fast amplifier, with slew rate of 11.5 V/μs and bandwidth of 240 kHz while driving the 2 nF piezo load. (This requires about 25 mA of current into each of the two electrodes.) However, in tests with an amplifier of slew rate 1.6 V/μs and bandwidth of 48 kHz, the motion threshold for the sawtooth was increased by about 40%, whereas that for the improved cycloid was increased by about 7%. Although the percentage increase is large, especially for the sawtooth, these thresholds are still easily attainable.

TABLE I. Motion threshold for three drive wave forms. The thresholds quoted in V are the minimum wave form peak voltages applied to one x electrode needed for motion. (The opposite voltage is simultaneously applied to the opposite x electrode.) The thresholds quoted in nm are calculated using Ref. 8, and are therefore approximate. The uncertainties quoted cover the span of measurements made at five sample sites.

Wave form	Threshold (V)	Threshold (nm)
Cycloid	29 ± 2	165
Improved cycloid	27 ± 1	160
Sawtooth	21 ± 2	120

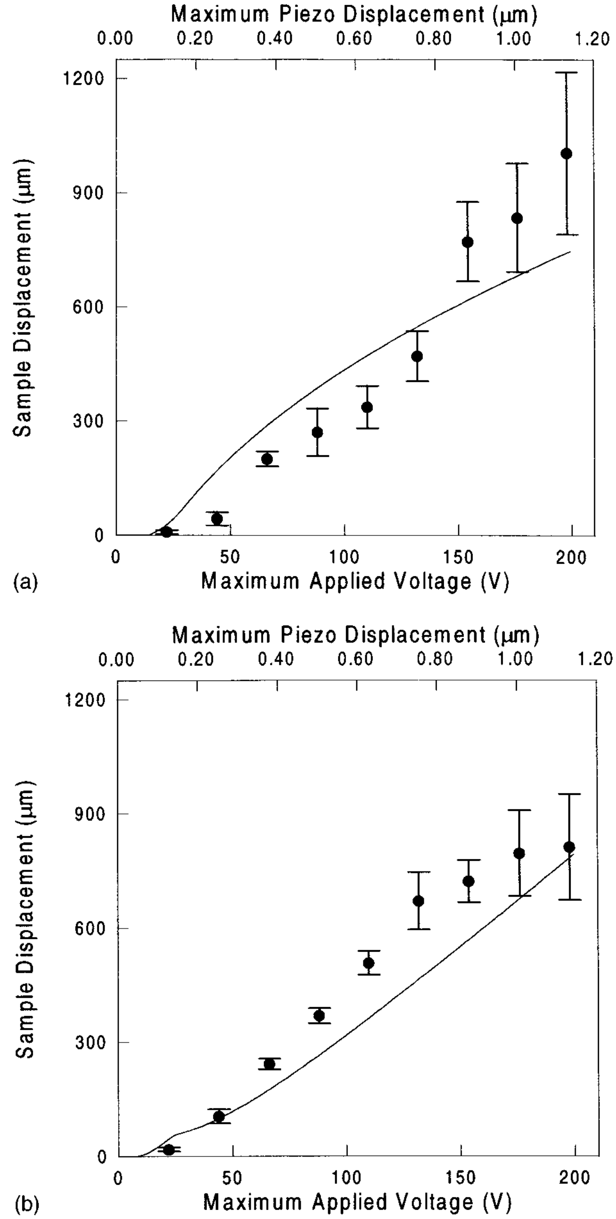

FIG. 5. (a) Sample displacement for 1000 steps vs drive wave form peak voltage for an improved cycloid with $Q=20$, cusp width of 614 μs, and delay between cusps of 614 μs. Solid circles: average of measurements taken at ten different sample sites for each voltage. The error bars represent 95% confidence intervals for the average of the ten measurements. Solid line: simulation with no adjustable parameters. The scale of the maximum piezo displacement is based on Ref. 8, and is therefore approximate. (b) Sample displacement for 1000 steps vs drive wave form peak voltage for a sawtooth with repeat frequency 813 Hz [same repeat frequency as in (a)]. Solid circles: average of measurements taken at ten different sample sites for each voltage. Solid line: simulation with no adjustable parameters.

Figures 5(a) and 5(b) show the sample displacement for a wave train of 1000 steps as a function of wave form amplitude for the improved cycloid and sawtooth wave forms, respectively. We noticed that, when working near the motion threshold, the sample would often move until it reached a region of higher friction and then stop. To then move it further in the same direction required a somewhat higher voltage. Therefore, while collecting the data for Fig. 5, the sample was moved about 1 mm by hand after every trial [i.e., it was moved 100 times for each of Figs. 5(a) and 5(b)], so that the data shown represent average sites on the sample, rather than sites of local maxima in the friction.

At amplitudes well above threshold, the amount of displacement is about the same for the two wave forms. The error bars for the sawtooth are somewhat smaller.

Also shown in Figs. 5(a) and 5(b) are the results of a simple computer simulation of the stick-slip process, with no adjustable parameters. In the simulation, the end of the piezo tube was treated as a damped simple harmonic oscillator that moves in response to the driving force provided by the applied wave forms, i.e., $m\ddot{x} = F_{\text{friction}}(t) + F_{\text{applied}}(t) - kx - b\dot{x}$, where x is the position of the end of the piezo, t is time, F_{friction} is the frictional force between the end of the tube and the sample, F_{applied} is the force resulting from the applied wave forms, k is the spring constant, and b is a damping constant. The only force acting on the sample was the frictional force from the end of the piezo tube. For the simulation, the mass of the moving end of the piezo tube was assumed to be the sum of the mass of the washer, magnet, etc. epoxied to the end of the tube, plus half the mass of the tube itself, for a total of 0.92 g. As previously mentioned, the mass of the sample (plus μ-metal plate) was 0.626 g, and the static frictional force was measured to be 0.065 ± 0.005 N. The kinetic frictional force was estimated by assuming that the ratio of kinetic to static frictional forces for the μ-metal plate sliding against the stainless-steel washer was the same as that for steel sliding on steel,[9] i.e., a ratio of kinetic/static $= 0.86$.

The lowest resonant frequency of the piezo with the sample was measured using the double piezoelectric effect,[10] and found[7] to be 9000 Hz. This is in excellent agreement with the value of 8900 Hz calculated from the known masses of the various components and the elastic constants of the piezo tube.[11] We used the measured value to calculate the spring constant used in the simulation.

Our piezo is heavily damped, as was recommended by Tiedje and Brown.[12] This damping is achieved by the ultramini-coax cable that runs through the center of the piezo tube, and that is firmly attached at the base of the piezo tube and to the disk magnet. The damping constant b used for the simulation was estimated to be 82 kg/s by comparing the height of the double-piezo resonance peak with the background.

Although the simulation does not correctly predict every detail of the observed behavior, the general agreement is remarkable, especially considering the simplicity of the model and the lack of adjustable parameters. Additionally, the simulation correctly predicts that the sawtooth should have the lowest motion threshold and that the threshold for the improved cycloid should be slightly lower than that for the standard cycloid. (However, the values predicted for these thresholds are about a factor of 2 lower than the observed values, perhaps because the simulation does not include the finite bandwidth of the wave form amplifier.)

The simulation also suggests why the improved cycloid is slightly better than the standard cycloid. The maximum acceleration of the end of the piezo tube does not occur exactly at the apex of either cycloidal wave form. Rather, as is expected for the response of a harmonic oscillator, the maximum acceleration is delayed (phase shifted). The maximum pseudoforce applied to the sample, therefore, occurs at the peak of the piezo displacement, rather than at the peak of the drive wave form. Because the improved cycloid has width and curvature that are more closely matched to the natural resonance of the end of the piezo, the improved cycloid excites a larger peak response at the end of the piezo than does the standard cycloid. For the sawtooth, as shown by the simulation, the end of the piezo experiences a very large acceleration at the sudden jump, much larger than the acceleration for either of the other wave forms. The acceleration in the opposite direction that occurs at the end of the jump is attenuated by the damped harmonic oscillator behavior, and is only about one-third as large as the initial acceleration.

Although the sawtooth wave form is the most effective for this $x-y$ translation system, it is important to note that it is not always the best choice for other types of stick-slip drives. For example, we and others[5] have observed that cycloidal wave forms are more effective for coarse z-approach systems in which a relatively massive ''wagon'' (>2 g) is driven along support rails.

VI. DISCUSSION

We have demonstrated a very simple system for long-range $x-y$ translation of SPM samples based on stick-slip motion of a magnetically held sample. We tested three drive wave forms: a sawtooth, a cycloid, and an ''improved'' cycloid. The improved cycloid provided slightly better performance than the standard cycloid, and is less demanding of the electronics than the sawtooth. Surprisingly, however, the sawtooth gave better performance than either cycloid, both for motion threshold and for consistency of step size. Very reliable motion was achieved with controllable step size ranging from 20 nm to 1 μm, and with maximum translation rate of about 0.8 mm/s. The system has the advantage that it impossible to accidentally drive the sample off the piezo. The field strength from the magnetic hold down is less than 100 G at the sample. This should cause no trouble for most samples, but, if necessary, could be considerably reduced by cutting the disk magnet in two and inverting one half. (This would create a tighter return path for the flux, but would still provide abundant hold-down force.)

A simple computer simulation based on a damped harmonic oscillator model for the piezo tube correctly predicted the general features of the observed behavior with no adjustable parameters. Clearly, the results of this model must be interpreted with caution, since it is much simpler than the actual physical apparatus, and does not correctly predict all details of the observed behavior. However, we anticipate that this model will be helpful in evaluating other possible drive wave forms and in providing guidance for the optimization of parameters. Our experimental results, together with the simulation, show that it is essential to consider the resonant response of the piezo when designing stick-slip translation systems and evaluating drive wave forms.

ACKNOWLEDGMENTS

The authors would like to thank their machinist Bruce Boyes, and acknowledge helpful discussions with Alex de Lozanne and C. K. Shih. This work was supported by the Research Corporation (Grant No. CC3400), by the Council for Undergraduate Research (AIURP) Student Summer Fellowship Program, and by the Zimmer Corporation.

[1] See, for example, C. J. Chen, *Introduction to Scanning Tunneling Microscopy* (Oxford University Press, New York, 1993), p. 242.
[2] Y. Kuk and P. J. Silverman, Rev. Sci. Instrum. **60**, 165 (1989).
[3] See, for example, R. R. Schlittler and J. K. Gimzewski, J. Vac. Sci. Technol. B **14**, 827 (1996), and references therein.
[4] A. Asenjo, A. Buendia, J. M. Gomez-Rodriguez, and A. M. Baro, J. Vac. Sci. Technol. B **12**, 1658 (1994).
[5] C. Renner, P. Niedermann, A. D. Kent, and Ø. Fischer, Rev. Sci. Instrum. **61**, 965 (1990).
[6] M. Okano, K. Kajimura, S. Wakiyama, F. Sakai, W. Mizutani, and M. Ono, J. Vac. Sci. Technol. A **5**, 3313 (1987).
[7] Some less pronounced resonances were observed at lower frequencies. Observations with a high-resolution optical microscope indicated that these were resonances in the scanning tunneling microscope base. Since motion at these frequencies would cause about 1/4 the acceleration as motion at the piezo fundamental frequency, and also for simplicity, these modes were left out of the simulation.
[8] C. J. Chen, Appl. Phys. Lett. **60**, 132 (1992).
[9] P. A. Tipler, *Physics for Scientists and Engineers*, 3rd ed. (Worth, New York, 1990), p. 110.
[10] C. J. Chen, Ultramicroscopy **42–44**, 1653 (1992).
[11] M. E. Taylor, Rev. Sci. Instrum. **64**, 154 (1993).
[12] T. Tiedje and A. Brown, J. Appl. Phys. **68**, 649 (1990).